Design of a Variable Reactor for Load Balancing and Harmonics Elimination

H. Dalvand, S. W. Su and Q. P. Ha
Faculty of Engineering, University of Technology, Sydney
Broadway, NSW 2007, Australia
Email: {hdalvand, steven.su, quangha}@eng.uts.edu.au

Abstract-This paper presents the design of a variable inductor with a rotational magnetic core whose position is controlled in a closed-loop system. This magnetic structure facilitates the impedance changes which may be used for load balancing, harmonics elimination, transient response improvement, and as a controlled reactor in static VAr compensation (SVC). The design of the inductor and analysis of its impedance change caused by positioning a movable element are carried out by using the finite element method. As a result, the variation range of the impedance is determined. The proposed variable inductor is compared with a typical SVC reactor. The results show good performances in static var compensation with higher reliability and no harmonics generated. For closed-loop control, a second-order sliding mode controller is designed for position control of the rotating core via a DC motor. Simulation results of the proposed system present highly robust and accurate responses without control chattering in face of nonlinearities and disturbances.

I. INTRODUCTION

The inductance of a variable reactor can be made adjustable by displacement of one of its magnetic parts. Several models and structures may be adopted for varying the reactor inductance, such as horizontal and vertical relocatable elements. It should be noted that displacement associated with vertical and horizontal movements of the core coupled to an actuator tends to be more complicated and slower than with a rotational movement. In this work, rotary displacement is suggested for a variable reactor so that its impedance changes with the same pace as that of harmonics, load, voltage and current unbalancing. Fig. 1 shows the proposed structure for such a variable inductor. The current enters from conductors 1, 3, and 5 and leaves respectively from conductor 2, 4, and 6 [1-3].
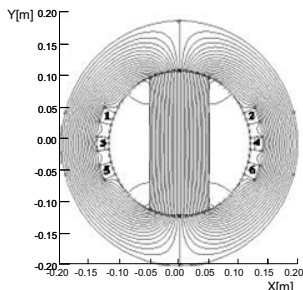

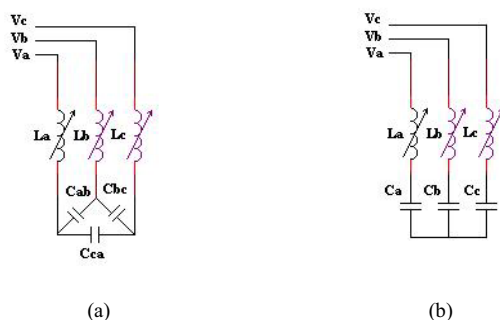Fig. 1. The proposed structure for a variable reactor

Fig. 2. The proposed structure for load balancing in delta (a) and star (b).

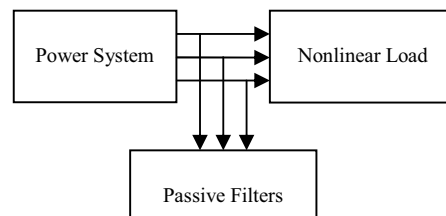Fig. 3. Series passive filter system (SFS)

Fig. 4. Parallel passive filter system (PFS).

II. VARIABLE INDUCTOR APPLICATIONS

A. Balancing the Three Phase Load

The proposed structure shown in Fig. 2(a) can be used for load balancing. For connection the proposed filter to the load, two possible implementations are possible, as presented in the Figures 3 and 4, where the delta connection of the capacitors in the passive filter results in three times lower capacitances than for the star connection, considering the same inductors and tuning frequency. Notably, although the voltage applied is higher than in the star connection, this can be considered as a partial advantage because the capacitors can handle more

reactive power for improvement of the power factor at the fundamental frequency.

If the compensating system is delta-connected, the magnitude of susceptance in each leg in a star connection can be obtained by applying the delta-star transform as:

$$B_\gamma^{ab} = \frac{1}{3\sqrt{3}V^2}\frac{1}{T}\int_0^T (v_{bc}i_{a(l)} + v_{ca}i_{b(l)} - v_{ab}i_{c(l)})dt$$

$$B_\gamma^{bc} = \frac{1}{3\sqrt{3}V^2}\frac{1}{T}\int_0^T (v_{ca}i_{b(l)} + v_{ab}i_{c(l)} - v_{bc}i_{a(l)})dt \quad (1)$$

$$B_\gamma^{ca} = \frac{1}{3\sqrt{3}V^2}\frac{1}{T}\int_0^T (v_{ab}i_{c(l)} + v_{bc}i_{a(l)} - v_{ca}i_{b(l)})dt.$$

With the delta-star transform, the proposed structure is converted to the star equivalence illustrated in Fig. 2 (b). In this system, the relationship between the capacitors of the two structures is given by:

$$C_a = \frac{C_{bc}C_{ca} + C_{ca}C_{ab} + C_{ab}C_{bc}}{C_{bc}}$$

$$C_b = \frac{C_{bc}C_{ca} + C_{ca}C_{ab} + C_{ab}C_{bc}}{C_{ca}} \quad (2)$$

$$C_c = \frac{C_{bc}C_{ca} + C_{ca}C_{ab} + C_{ab}C_{bc}}{C_{ab}}$$

Finally the impedance of each leg is obtained by using the calculated susceptance of delta legs as:

$$Z_a = \frac{B_{bc}}{B_{bc}B_{ca} + B_{ca}B_{ab} + B_{ab}B_{bc}} = X_{La} - X_{Ca}$$

$$Z_b = \frac{B_{ca}}{B_{bc}B_{ca} + B_{ca}B_{ab} + B_{ab}B_{bc}} = X_{Lb} - X_{Cb} \quad (3)$$

$$Z_c = \frac{B_{ab}}{B_{bc}B_{ca} + B_{ca}B_{ab} + B_{ab}B_{bc}} = X_{Lc} - X_{Cc}$$

So by measuring the phase voltage and current, the magnitudes of the proposed system impedances need to be adjusted in order to balance the three-phase load and to compensate for the reactive power. Further details for this are reported in [4].

B. Self-Tuning Harmonic Filter

Because of the load variations, voltage and current harmonics are variable, so single tuned filters cannot eliminate the harmonics completely, therefore these filters do not always operate with a maximum efficiency at a time. The resonance frequency of single tuned filters also changes due to voltage variation and ageing. So they loose their initial performance in absorbing the harmonics. Indeed, the generated reactive power of the capacitors and in turn their impedance is reduced by ageing. Moreover, series inductance of transformers changes by voltage variations as well. Due to these effects, the resonance frequency of the filter may change.

The disadvantages of passive filters can be overcome by utilising a variable inductor which can change the resonance frequency to achieve the best performance. Moreover, they are preferred to active filters because active filters cause harmonics resulting from switching operations, and they are expensive due to the use of high rating switches. The quality factor and resonance frequency of the filter are given by

$$Q_a = \frac{X_{La}}{R_a}, f_r = \frac{\omega}{2\pi\sqrt{X_{La}/X_{Ca}}} \quad (4)$$

whose values can be changed by adjusting the system inductance. By considering a target function, e.g. current total harmonic distortion (THD), it is possible to change the inductance so that it operates optimally [5].

For the proposed magnetic structure shown in Fig. 1 for a thickness of 30 cm, the potential and electromagnetic poles in 0^0 and 90^0 rotation respectively can be illustrated in Fig. 5 by using the finite element method (FEM) with the Vector Field software.

The flux and flux density distributions obtained from FEM are depicted in Fig. 6. By connecting a 380V power supply to the inductor, the FEM simulation is carried out with the use of Vector Field. From the flowing current obtained with respect to different core angles, the resistance remains unchanged at 0.324 • but the structure inductance values vary correspondingly and are recorded in Table I.

Therefore, the proposed inductor has an inductance varying between 22 and 92 mH. This inductor can be used in many applications which will be discussed later.
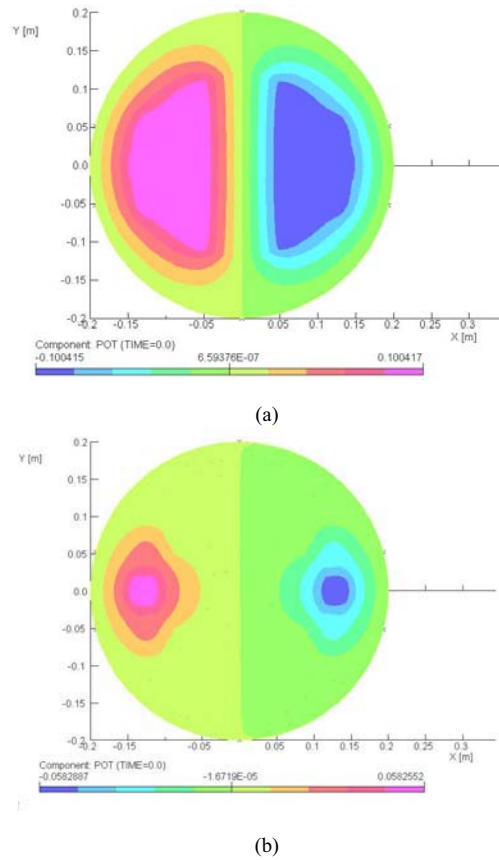

(a)

(b)

Fig. 5. The generated potential and electromagnetic poles respectively in 0^0 (a) and 90^0 (b) rotation.

INDUCTANCE OF PROPOSED INDUCTOR VERSUS CORE ROTATION

Core rotation (degree)	0	30	60	90
Inductance (mH)	92.33	91.36	60.73	21.99

The variable inductance of the structure is a function of the current, $i(t)$, and the core rotary position, $\theta(t)$, so the co-energy stored in the structure is:

$$W_m = \frac{1}{2} L(i, \theta)(i(t))^2. \qquad (5a)$$

By differentiating (5a), the electromagnetic torque is calculated as

$$T_m = \frac{\delta W_m}{\delta \theta} = \frac{1}{2} i^2 \frac{dL(i, \theta)}{d\theta}. \qquad (5b)$$

III. COMPARISON OF THE PROPOSED INDUCTOR WITH STATIC VAR COMPENSATOR

The proposed system is compared with a static var compensator (SVC). The SVC is simulated by PSPICE software in which thyristor controlled reactors (TCR) are modelled by thyristor switches. In order to maintain similarity with the proposed system, the inductor capacity used in the TCR is set equal to 90 mH with the same supply voltage of 380V. The SVC is simulated for different firing angles.

A. Harmonics Generation

The SVC generates harmonics because of switching elements in the TCR. From the current harmonics shown in Fig. 7, the 5th harmonic component can reach 5 percent of the current in 0^0 firing angle.

Several investigations have been done on harmonics reduction in SVCs. For example, using 12-pulse compensator is one of the solutions but due to a high cost, it is not practical.

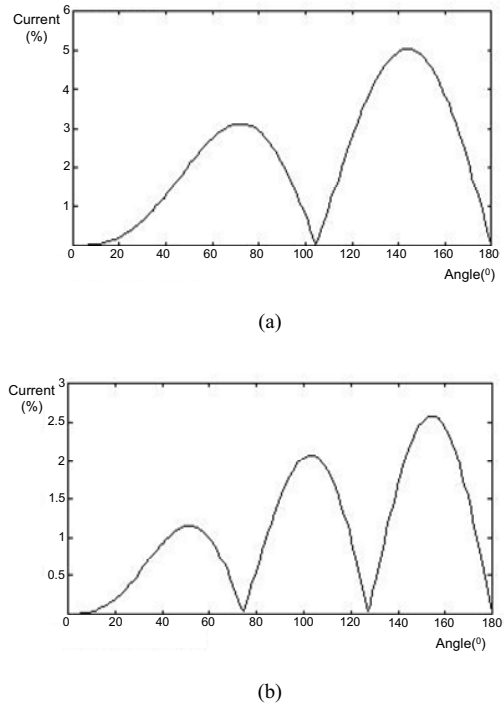
Fig. 6. The generated flux and flux density respectively in (a-b) 0^0, (c-d) 30^0, (e-f) 60^0 and (g-h) 90^0 rotation.

(a)

(b)

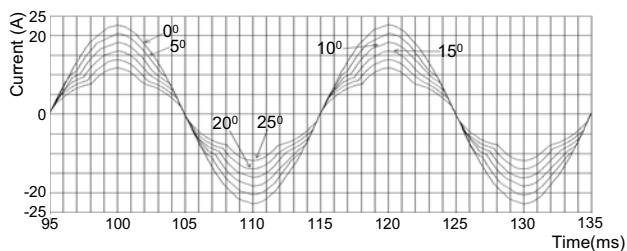Fig. 7. The current harmonics of the SVC at 0^0 firing angle: (a) 5th and (b) 7th.

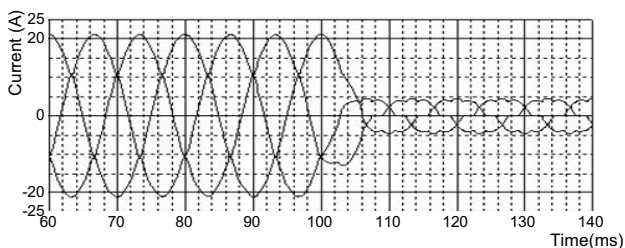Fig.8. The phase current, inductor current and their harmonics of simulated compensator in firing angles 5^0 to 25^0

Fig. 9. The transient condition for firing angle transmitting from 5^0 to 45^0

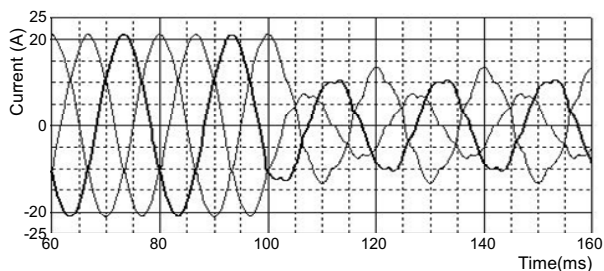Fig. 10. The transient condition for firing angle transmitting from 5^0 to 15^0, 30^0 and 45^0

The common solution is to use filters with the SVC to reduce harmonics. It should be noted that if the SVC does not generate harmonics, it is possible to absorb more harmonics from the power system. In other words, since the current flowing through the filter reaches a certain value, by absorbing the compensator harmonics, some of its capacity to absorb the power system's reactive and harmonics currents is reduced. In [6], a comprehensive analysis of the compensator harmonics is presented. Here, for more thorough interpretation, the compensator model has been simulated by using the PSPICE software.

Figure 8 shows the results of simulated compensator in firing angles from 5^0 to 25^0. This simulation contains the phase current, inductor current and their harmonics. It is clear that the amount of harmonics increases by increasing firing angle. However, there are the 3rd harmonic in the SVC inductor current which does not appear in the phase current because of system symmetry and its delta structure.

B. Three Phase Load Balancing

Both the proposed system and SVC can balance the load while the former model does not produce harmonics as it does

not utilise active elements. However, it should be noted that in addition to harmonics discussed before, SVC does generate the 3rd harmonics as well [7, 4].

C. Response Time

It is known that SVC can perform static VAr compensation within half cycle, independent of the balanced and unbalanced load. According to the simulation results shown in Fig. 9, by changing the firing angle from 5^0 to 45^0, the output current changes quickly within half cycle. In this simulation, the firing angle is 5^0 during the first 5 cycles and it is changed to 45^0 in the second 5 cycles.

Moreover, the output current of compensator becomes unbalanced rapidly within the half cycle by changing the firing angle from 5^0 to 15^0, 30^0 and 45^0, shown in Fig. 10. In this simulation, the firing angle is 5^0 during the first 5 cycles and it changes to 15^0, 30^0 and then 45^0 during the second 5 cycles. It should be noted that because the SVC is usually connected to the power system with a separate transformer or it is installed in the tertiary of a power transformer, the compensator currents transmission to the transformer secondary side is delayed because of its impedance [8]. Usually this delay increases the compensation time to 1.5 cycles. Our proposed system may have a higher time constant because of the mechanical time constant. But for most types of loads, load variation time is more than 10 seconds. Therefore the proposed system can be useful for compensation for static VAr.

D. The Need for Peripheral Equipment and Compatibility to Different Voltage Levels

Using power thyristors with high ratings for low voltage applications is not economical. Due to this fact, in practice, SVCs are utilized in voltage levels above 20 kV. The proposed compensator, not containing thyristors, is suggested to be used in different voltage levels without any limitation or additional peripheral devices, provided that some sufficient insulation is maintained [8].

E. Equipment Cost

SVCs are costly due to the use of high power thyristors in their structure, protection and cooling system, and firing angle control equipment. The proposed compensator, not using solid state switches and not requiring other maintenance considerations and equipment, shall be implemented with much less cost compared to an SVC.

F. Energy Saving

SVC increases the current losses because of the harmonics generated. Furthermore, the switching losses which amount to 1% of the total power are also considerable. The SVC can perform effective compensation in high voltage levels, therefore imbalance and generation harmonics should be compensated for in the high voltage side instead of its generating source. Consequently the SVC causes power loss in low voltage side and hence increases energy consumption.

Also since SVC is connected to the network via a power transformer, the generated harmonics cause increased eddy current and conductive losses. The proposed compensator, while being able to absorb harmonics, does not generate any harmonics itself.

G. Modular Installation and Expansion

Having a modular and expandable structure is a merit of a system. In many instances, the capacity of a compensation system or its characteristics should be increased due to changes that occur in the load. An SVC does not have the modular expansion capability since all the active devices and the connecting transformer are designed for the nominal values and paralleling two SVCs requires many critical considerations which may make it hardly practical for many applications. In contrast, the proposed system can possess a modular and expandable structure and the user can easily adapt the system by adding other modules.

IV. SYSTEM DESCRIPTION AND DYNAMIC EQUATION

A block diagram of the position control system for closed-loop control of the movable core is shown in Fig. 11. In this figure, reference position θ_{ref}, obtained from the required value for the reactor inductance, is compared with the actual angle θ, measured from an absolute encoder. The position error is the inputs to the sliding mode controller block. The command voltage signal is the output of the controller.

The motor can be described by the following state equations:

$$\omega = \frac{d\theta}{dt}$$
$$J\frac{d\omega}{dt} = K_T i_a - T_L(t) - B\omega - K\theta \tag{6}$$
$$u(t) = K_E \omega + R_a i_a + L\frac{di_a}{dt},$$

where i_a is the armature current (A), ω is the angular speed (rad/s), θ is the angular position (rad) and T_L the total mechanical load torque (N.m), including T_m given in (5a). The control voltage u is the armature voltage (V). Other system parameters are listed as R_a for the total armature resistance (1.2 Ω), L_a for the armature inductance plus the smoothing inductance (0.01 H), B for the total mechanical damping (0.011 N.m.s), J for the total moment of inertia (0.208 Kg.m^2), K_T (0.3 N.m/A), K_E (0.3 volt/rad sec^{-1}) and K (0 N.m/rad) for motor constants.

The control system to be implemented includes a power amplifier, a DC motor, a tachometer as the speed sensor, a potentiometer as the position sensor, and a data acquisition unit to display real-time system outputs on a PC monitor. Choosing the system states as

$x_1 = \theta,$

$x_2 = \omega = \frac{d\theta}{dt},$

$x_3 = i_a$

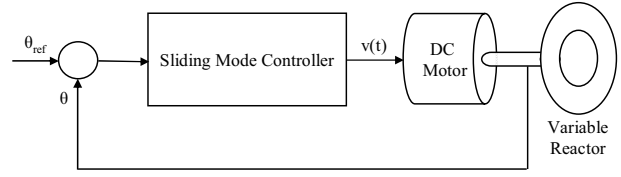the state space equation of system can be established as:

Fig. 11: Block Diagram of the DC motor with sliding mode controller

$$\dot{\mathbf{x}} = \begin{bmatrix} 0 & 1 & 0 \\ a_1 & a_2 & a_3 \\ 0 & a_4 & a_5 \end{bmatrix}\mathbf{x} + \begin{bmatrix} 0 \\ 0 \\ b_1 \end{bmatrix}u(t)$$
$$+ \begin{bmatrix} 0 \\ d_1 \\ 0 \end{bmatrix}T_L(t) \tag{7}$$
$$y = \begin{bmatrix} 1 & 0 & 0 \end{bmatrix}\mathbf{x}$$
$$\mathbf{x} = \begin{bmatrix} x_1 & x_2 & x_3 \end{bmatrix}^T,$$

where $a_1 = -\frac{K}{J}$, $a_2 = -\frac{B}{J}$, $a_3 = \frac{K_T}{J}$, $a_4 = -\frac{K_E}{L}$, $a_5 = -\frac{R_a}{L}$,

$b_1 = \frac{1}{L}$, and $d_1 = -\frac{1}{J}$.

V. SLIDING MODE CONTROLLER DESIGN

Here the sliding mode theory is adopted to yield robust positioning performance [9].

For this, let us define a sliding function

$$\sigma = \ddot{e} + 2\xi\omega_n \dot{e} + \omega_n^2 e = \ddot{e} + \lambda_1 \dot{e} + \lambda_2 e \tag{8}$$

from desired values of natural frequency ω_n and damping

ratio ξ: $\begin{cases} \omega_n = \sqrt{\lambda_2}, \xi = \dfrac{\lambda_1}{2\sqrt{\lambda_2}} \\ \qquad or \\ \lambda_2 = \omega_n^2, \lambda_1 = 2\xi\omega_n. \end{cases}$

With time derivatives

$$\dot{\sigma} = \dddot{e} + \lambda_1 \ddot{e} + \lambda_2 \dot{e} \tag{9}$$

$e = x_1 - x_{1\_ref}$ $\dot{e} = x_2 - \dot{x}_{1\_ref}$

$\ddot{e} = a_1 x_1 + a_2 x_2 + a_3 x_3 + d_1 T_L - \ddot{x}_{1\_ref}$

$\dddot{e} = a_1 \dot{x}_1 + a_2 \dot{x}_2 + a_3 \dot{x}_3 + d_1 \dot{T}_L - \dddot{x}_{1\_ref}$

$\dot{\sigma} = Ax_1 + Bx_2 + Cx_3 + Du + f_d(t) - \phi_{ref}$

where

$\begin{cases} A = a_1 a_2 + \lambda_1 a_1 \\ B = \lambda_2 + \lambda_1 a_2 + a_3 a_4 + a_2^2 + a_1 \\ C = \lambda_1 a_3 + a_3 a_5 + a_2 a_3 \\ D = a_3 b_1 \end{cases}$

$f_d(t) = (\lambda_1 d_1 + a_2 d_1)T_L + d_1 \dot{T}_L, \phi_{ref} = \lambda_2 \dot{x}_{1\_ref} + \lambda_1 \ddot{x}_{1\_ref} + \dddot{x}_{1\_ref}$

the control output $u(t)$ can be designed to consist of two

components, namely, u_{Eq} an equivalent control and u_{Sw} a switching control, i.e.

$$u = u_{Eq} + u_{Sw}. \tag{10}$$

The equivalent control u_{Eq} is determined by the desired dynamics of the system in the sliding mode and the switching control u_{Sw} is to compensate for uncertainties and disturbances such that the system state is driven towards the sliding surface (reaching phase).

To obtain the equation for equivalent part, the sliding variable should be constant in nominal condition which means:

$$\dot{\sigma}\Big|_{\text{nominal condition}} = 0 \Leftrightarrow Ax_1 + Bx_2 + Cx_3 + Du_{Eq} - \phi_{ref} = 0 \tag{11}$$

Therefore;

$$u_{Eq} = \frac{1}{D}(Ax_1 + Bx_2 + Cx_3 - \phi_{ref}).$$

For the switching part, by considering the Lyapunov function:

$$V = \frac{1}{2}\sigma^2 \tag{12}$$

$$\dot{V} = \sigma\dot{\sigma}$$

$$\dot{V} = \sigma(Ax_1 + Bx_2 + Cx_3 + Du_{Eq} + f_d(t) + D(u_{Eq} + u_{Sw}) - \phi_{ref})$$
$$= \sigma(f_d(t) + Du_{Sw})$$

By assuming

$$\|f_d(t)\| < F \qquad \forall t \tag{13}$$

$$\dot{V} < -\gamma|\sigma| \Rightarrow |\sigma(t)| \le \varepsilon_0 e^{-\gamma t} \tag{14}$$

and selecting the gain

$$K = \frac{F + \gamma}{|D|} \tag{15}$$

one can derive

$$u_{Sw} = -K|\sigma|sign(\sigma) \tag{16}$$

The system dynamic responses for a reference position trajectory signal simulated with Matlab/Simulink are shown in Fig. 12.

In this simulation, a pulse signal is applied to the system in time 2.5 second as disturbance. However the performance of the controller can be observed. Moreover, according to the results, the proposed controller has a very small rise time (less than 0.5 second), settling time (about 0.8 second) and overshoot (about 8%) for different angles.

VI. CONCLUSION

In this paper we have presented the design of a variable reactor whose impedance changes with the variation of a relocatable rotary element. This inductor can be used for VAr compensation and load balancing. In such applications important performances by using the proposed compensator is compared with the use of SVCs. A sliding mode controller is designed for closed-loop control of the movable core positioning. Robustness of the control system is verified through simulation.
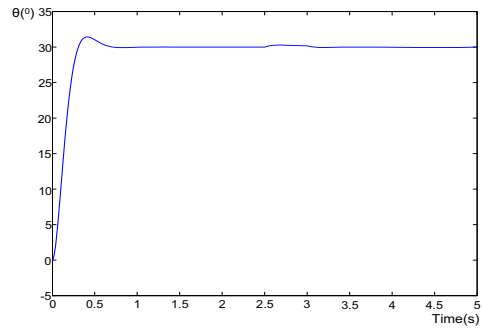

Fig. 12: Position responses of the simulated system for angle 30^0.

VII. REFERENCES

[1] H. Oka, and P.P. Biringer, "Control characteristic analysis of a ferrite orthogonal core," *IEEE Trans. Magnetics*, vol. 26, pp. 2888-2893, 1990.

[2] H. Oka, F.P. Dawson., T. Sakuta, and J.D. Lavers, "Magnetic fluid based variable inductors for inductively coupled plasma applications," *IEEE Trans. Magnetics*, pp. 4175-4177, 1995.

[3] S. Rahmani, K. Al-Haddad, and H.Y. Kanaan, "A comparative study of shunt hybrid and shunt active power filters for single-phase applications: Simulation and experimental validation," *Maths. and Computer in Simulation,* vol. 71, pp. 345-359, 2006.

[4] H. Dalvand, M.T. Nguyen, N. M. Kwok, and Q. P. Ha, "A new hybrid filter for power quality improvement in unbalanced load conditions," *Proc. 10th Int. Conf. on Control, Automation, Robotics and Vision*, Hanoi Vietnam, 17-20Dec. 2008, to appear.

[5] S. Rahmani, K. Al-Haddad, and F. Fnaiech, "A new PWM control technique applied to three phase shunt hybrid power filter," *Proc. IEEE Int. Conf. Ind. Electro. (IECON'02)*, Spain, vol. 1, pp. 727- 732, 2002.

[6] K. Wilkosz, M. Sobierajski, and W. Kwasnicki, "The analysis of harmonic generation of SVC and STATCOM by EMTDC/PSCAD simulations," *Proc. 8th Int. Conf. on Harmonic and Quality of Power ICHQP'98*, Greece, vol. 2, pp. 853-858, 1998.

[7] S. Y. Lee and C. J. Wu, "Reactive power compensation and load balancing for unbalanced three-phase four-wire system by a combined system of an SVC and a series active filter," *IEE Proc.-Electr. Appl.*, vol. 147, no. 6, pp. 563-570, 2000.

[8] D.J. Hanson, C. Horwill, B.D. Gemmell, and D.R. Monkhouse, "A STATCOM-Based Relocatable SVC Project in the UK for National Grid," *Proc. IEEE Power Engineering Society Winter Meeting*, NewYork, USA, 2002, pp. 532-537.

[9] A. Sabanovic, L. Fridman, and S. Spurgeon, *Variable Structure Systems: from Principles to Implementation.* series 66, IEE: London, UK, 2004.